In situ jet energy calibration in the ATLAS experiment.

C. Biscarat, R. Lefevre, C. Santoni

HAL Id: in2p3-00007124

http://hal.in2p3.fr/in2p3-00007124

Submitted on 1 Dec 2000

IN SITU JET ENERGY CALIBRATION
IN THE ATLAS EXPERIMENT

Catherine Biscarat, Régis Lefèvre, Claudio Santoni

Laboratoire de Physique Corpusculaire, 63177 Aubière Cedex, France

Presented by Régis Lefèvre on behalf of the ATLAS Collaboration

ABSTRACT

For precision measurements, like the top mass determination, the purpose of the ATLAS experiment is to know the absolute jet energy scale at a level of 1%. Using only test-beam data, systematic uncertanties are of the order of 5 to 10% (dead material, fragmentation modelling...). *In situ* calibrations are then needed. Preliminary results using charged isolated hadrons and $Z^\circ + jet$ events are presented here.

1 E/p **calibration**

This method is based on charged isolated hadrons ($\pi^\pm$ or $K^\pm$) and makes use of precise momentum (p) measurements in the tracker. The calibration can be achieved using E/p ratio where E is measured in the calorimeters. This method allows direct comparison with test-beam results and inter-calibration

of calorimeters of different technologies. The η coverage is limited by the inner detector ($|\eta| < 2.5$). High single hadron rate come from τ decays *via* vector boson production

- $W^{\pm}(+jets) \to \tau^{\pm}\nu_{\tau}(+jets)$ with $\tau^{\pm} \to h^{\pm}\nu_{\tau}$,

- $Z^{\circ}/\gamma^{*}(+jets) \to \tau^{+}\tau^{-}(+jets)$ with at least one $\tau^{\pm} \to h^{\pm}\nu_{\tau}$.

The main backgrounds are QCD events and τ decays themselves (multi-prongs, π° production).

1.1 Event selection

1.1.1 On line selection

The event selection is first based on the choice of a specific preliminary level 1 trigger for hadronic τ decays consisting in one τ-jet candidate of transverse momentum greater than $20 GeV/c$ and a missing transverse energy greater than $30 GeV$. The efficiency of $Z^{\circ}/\gamma^{*} \to \tau^{+}\tau^{-}$ channel is increased using also lepton triggers: isolated electron or muon of transverse momentum greater than $20 GeV/c$.

1.1.2 Pre-selection

A pre-selection is performed requiring at least one jet, no more than two jets or no more than one jet if there is one isolated lepton, no more than one isolated lepton and no isolated photon.

1.1.3 τ-jet selection

The selection demands to have a jet candidate with transverse momentum greater than $20 GeV/c$ in the inner detector acceptance. All the tracks in a cone centred on the jet direction and of size $\Delta R = 0.15$ in the (η, ϕ) plane are considered as matching tracks. The selection then requires at least one matching track with p_T greater than $25 GeV/c$.

1.1.4 Single track selection

Looking in a $\Delta R = 0.4$ cone around the hardest matching track, the isolation criterium rejects events with more than one additionnal track, or with one additionnal track of p_T above $1 GeV/c$.

Table 1: *Expected events (in millions) after the different selection steps for an integrated luminosity of $10\,fb^{-1}$.*

selection step	signal	$\tau^{\pm}$ background	QCD background
trigger	3.30	13.3	6000
pre-selection	2.66	11.9	1300
τ-jet	1.53	2.00	29
single track	1.31	1.14	0.13

1.2 Results

Tab.1 shows the selection results obtained with a fast simulation [1] study. The QCD rejection is very good and its final contribution represents only 10% of the signal one. Nevertheless, the residual $\tau^{\pm}$ decay background is of the order of the signal. This is essentially due to π° contamination representing more than 80% of this background after the final selection. The E/p distribution is shown in fig.1. Residual background introduces a shift on E/p mean value of the order of +4%.

1.3 Conclusions

This E/p calibration analysis shows that there is a good rejection of multi-tracks backgrounds. The level of neutral pion contamination is still too high. The possibility of π° rejection using the fine η strips of the first layer of the electromagnetic calorimeter has to be studied using a full simulation of showers development.

2 Jet energy calibration using $Z^{\circ} + jet$ events

To improve resolution and linearity, an *in situ* calibration of jet energy using events $q + g(\overline{q}) \rightarrow Z^{\circ} + q(g)$ with $Z^{\circ} \rightarrow e^{+}e^{-}$ or $\mu^{+}\mu^{-}$ was studied. Easy to trigger and to select, this channel benefits of huge statistics, and large η and energy coverages. It also allows independent b-jet energy calibration. Due to the high precision of Z° reconstruction, the calibration is performed using the tranverse momentum constraint: $p_T(jet) = p_T(Z^{\circ})$. Results reported here were obtained using full simulated events (limited to $|\eta^{jet}| \leq 1.2$, low luminosity case). Systematic errors were studied with a fast simulation program [1].
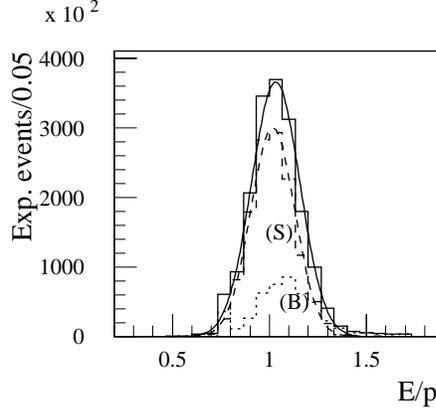
Figure 1: *E/p expected distribution for an integrated luminosity of* $10 fb^{-1}$ *after final selection. (S) signal events, (B) background events.*

2.1 Calibration procedure

2.1.1 *Step 1*

The calibration procedure is divided in 3 steps. In a first step the reconstructed energy is expressed as a function of the energies of cells associated to the jet, E_{cell}^{jet}'s, using electromagnetic scale calibration, and of calibration parameters

$$E_T^{rec}(jet) = \frac{f(a_l, E_{cell}^{jet})}{cosh(\eta^{jet})} \qquad (1)$$

These a_l's are then obtained for each interval in the $(p_T(Z^\circ), \eta^{jet})$ plane by minimising

$$\sum_{jet} \left(E_T^{rec}(jet) - p_T(Z^\circ)\right)^2 + \alpha \sum_{jet} \left(E_T^{rec}(jet) - p_T(Z^\circ)\right) \qquad (2)$$

This is equivalent to minimise the width of the transverse energy resolution constraining the Z° transverse momentum to be reproduced in mean value.

2.1.2 *Step 2*

In a second step, in order to be able to reconstruct jet energies without any *a priori* knowledge, linear interpolations of a_l's are performed as functions of jet transverse energy obtained using electromagnetic scale calibration $E_T(jet)$.

Table 2: *Mean value μ_Z and standard deviation σ_Z of gaussian functions fitting the $\{E_T^{rec}(jet) - p_T(Z^\circ)\}/p_T(Z^\circ)$ distributions.*

$p_T(Z^\circ)$ (GeV/c)	μ_Z (%)	σ_Z (%)
$40 - 60$	-1.9 ± 0.8	17.2 ± 0.7
$60 - 100$	-0.4 ± 0.8	16.3 ± 0.8
$100 - 200$	1.3 ± 0.8	9.3 ± 0.7
$200 - 300$	0.4 ± 0.4	7.5 ± 0.4

2.1.3 Step 3

In a final step, corrections based on simulation are applied to take into account residual unbalance due to initial state radiations (ISR).

2.2 Event selection

To reduce the unbalance between parton and Z° produced by ISR, the selected topologies have one and only one jet back-to-back with the Z° in the transverse plane. The cuts are: only one jet with $E_T(jet) \geq 15GeV$, $E_T(jet) \geq 20GeV$, $|\phi^{jet} - \phi^{Z^\circ} - \pi| \leq 0.15$, and $|M^{Z^\circ} - 91.187GeV/c^2| \leq 10GeV/c^2$.

2.3 Results

2.3.1 Step 1 results

The choosen parameterisation of the reconstructed energy is

$$\sum_{cells \in EM} \left(a_{EM} + \frac{b_{EM}}{|E_{cell}^{jet}|} \right) E_{cell}^{jet} + \sum_{cells \in HAD} \left(a_{HAD} + \frac{b_{HAD}}{|E_{cell}^{jet}|} \right) E_{cell}^{jet}$$
$$+ c\sqrt{E_{ACCB3}^{jet} E_{TILE1}^{jet}} + E_P^{jet} + E_{TS}^{jet} \qquad (3)$$

The two first terms allow to correct for non compensation of electromagnetic and hadronic calorimeters respectively [2]. The shape has been demonstrated in test-beam and is reproduced by the simulation [3]. The third term takes into account the energy lost in the barrel cryostat. Presampler and tile scintillators energies are not corrected. Tab.2 shows the obtained linearities and resolutions.
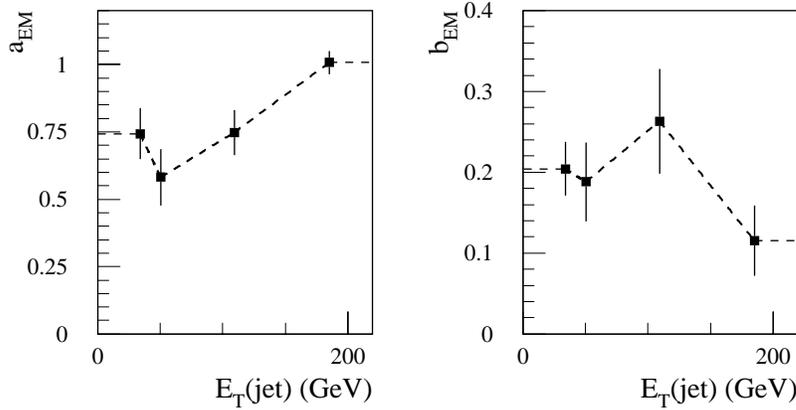
Figure 2: *Evolutions of parameters a_{EM} and b_{EM} for $0 \le |\eta^{jet}| \le 0.3$. Dashed lines represent the linear interpolations used in the analysis.*

Table 3: *Mean value μ_p^i (μ_p) and standard deviation σ_p^i (σ_p) of gaussian functions fitting the $\{E_T^{rec}(jet) - p_T(parton)\}/p_T(parton)$ distributions obtained using the interpolation of calibration parameters (the knowledge of $p_T(Z^\circ)$).*

$p_T(parton)$ (GeV/c)	μ_p^i (%)	σ_p^i (%)	μ_p (%)	σ_p (%)
$40 - 60$	0.0 ± 0.7	15.3 ± 0.6	0.6 ± 0.8	15.4 ± 0.7
$60 - 100$	2.2 ± 0.6	12.5 ± 0.6	1.8 ± 0.7	12.6 ± 0.7
$100 - 200$	0.8 ± 0.5	7.2 ± 0.5	1.3 ± 0.6	7.7 ± 0.5
$200 - 300$	0.8 ± 0.3	5.3 ± 0.2	0.9 ± 0.3	5.7 ± 0.3

2.3.2 Step 2 results

Tab.3 shows that the results obtained with the interpolation method are very closed to the ones obtained using the $p_T(Z^\circ)$ knowledge (step 1). This is due to the smooth evolution of calibration parameters as a function of the energy (see the examples of fig.2).

2.3.3 Step 3 results

To get μ_p^i and σ_p^i from the measurable quantities μ_Z and σ_Z, the two equations $\mu_p^i = \mu_Z + (\mu_p^i - \mu_Z)_{MC}$ and $\sigma_p^i = \sigma_Z \times (\sigma_p^i/\sigma_Z)_{MC}$ can be used in order to reduce systematic errors. Tab.4 shows that the resolution with respect to

Table 4: *Correction terms obtained with the actual Monte Carlo.*

$p_T(parton)$ (GeV/c)	$(\mu_p^i - \mu_Z)_{MC}$ (%)	$(\sigma_p^i/\sigma_Z)_{MC}$ (%)
$40 - 60$	1.9 ± 1.1	89 ± 6
$60 - 100$	2.6 ± 1.0	77 ± 5
$100 - 200$	-0.5 ± 0.9	77 ± 9
$200 - 300$	0.4 ± 0.5	70 ± 5

the Z° is clearly affected by the residual p_T unbalance. It also seems that the desired 1% level of accuracy on the determination of the jet energy scale can not be achieved without using these corrections. This is confirmed by the fast simulation results that exhibit corrections on linearity of 4.9, 1.5, and 0.4% from low to high p_T ranges.

2.4 Systematic uncertainties and conclusions

Uncertainties on foreseen Monte Carlo linearity corrections have been studied using a fast simulation and considering imperfect modelling of back-to-back topologies and of ISR. The results show that it would be possible to control the jet energy scale at the desired 1% level for transverse energies greater than $40 GeV/c$.

3 Acknowledgements

References

1. E. Richter-Was, D. Froidevaux, L. Poggioli, ATLFAST 2.0 a fast simulation package for ATLAS, ATLAS Internal Note ATL-PHYS-98-131 (1998).

2. W. Braunschweig *et al* (H1 calorimeter group), Nucl. Instr. Meth. **A265**, 246 (1988).

3. ATLAS Collaboration, ATLAS Detector and Physics Performance Technical Design Report CERN/LHCC/99-14, 266 (1999).